NREL
NATIONAL RENEWABLE ENERGY LABORATORY

Acoustic Array Development for Wind Turbine Noise Characterization

S. Buck
University of Colorado Boulder

J. Roadman and P. Moriarty
National Renewable Energy Laboratory

S. Palo
University of Colorado Boulder

NREL is a national laboratory of the U.S. Department of Energy
Office of Energy Efficiency & Renewable Energy
Operated by the Alliance for Sustainable Energy, LLC.

This report is available at no cost from the National Renewable Energy Laboratory (NREL) at www.nrel.gov/publications.

Technical Report
NREL/TP-5000-60457
November 2013

Contract No. DE-AC36-08GO28308

NREL
NATIONAL RENEWABLE ENERGY LABORATORY

Acoustic Array Development for Wind Turbine Noise Characterization

S. Buck
University of Colorado Boulder

J. Roadman and P. Moriarty
National Renewable Energy Laboratory

S. Palo
University of Colorado Boulder

Prepared under Task No. WE11.0315

National Renewable Energy Laboratory
15013 Denver West Parkway
Golden, CO 80401
303-275-3000 • www.nrel.gov

Technical Report
NREL/TP-5000-60457
November 2013

Contract No. DE-AC36-08GO28308

This report is available at no cost from the National Renewable Energy Laboratory (NREL) at www.nrel.gov/publications.

Available electronically at http://www.osti.gov/bridge

Available for a processing fee to U.S. Department of Energy and its contractors, in paper, from:

U.S. Department of Energy
Office of Scientific and Technical Information
P.O. Box 62
Oak Ridge, TN 37831-0062
phone: 865.576.8401
fax: 865.576.5728
email: mailto:reports@adonis.osti.gov

Available for sale to the public, in paper, from:

U.S. Department of Commerce
National Technical Information Service
5285 Port Royal Road
Springfield, VA 22161
phone: 800.553.6847
fax: 703.605.6900
email: orders@ntis.fedworld.gov
online ordering: http://www.ntis.gov/help/ordermethods.aspx

Cover Photos: (left to right) photo by Pat Corkery, NREL 16416, photo from SunEdison, NREL 17423, photo by Pat Corkery, NREL 16560, photo by Dennis Schroeder, NREL 17613, photo by Dean Armstrong, NREL 17436, photo by Pat Corkery, NREL 17721.

Printed on paper containing at least 50% wastepaper, including 10% post consumer waste.

Acknowledgments

The acoustic array design and testing team would like to acknowledge Scott Wilde and his operations team for their support in setting up, testing, and maintaining our equipment. Arlinda Huskey's help in supporting the program's logistics is much appreciated. Andy Scholbrock has been invaluable in coordinating availability of the Controls Advanced Research Turbine (CART)-2. Mike Asheim's input in array design, construction, and associated acoustic testing was also very useful. Finally, the project would not have been possible without the cooperation of the University of Colorado Boulder, their facilities, and the education they provide.

Nomenclature

BJT	bipolar junction transistor
CART-2	Controls Advanced Research Turbine (two-bladed)
CMM	coordinate-measuring machine
DAS	data acquisition system
FFT	fast Fourier transform
NI	National Instruments
NREL	National Renewable Energy Laboratory
NWTC	National Wind Technology Center
PSF	point spread function
RTV	room temperature vulcanization
SNR	signal-to-noise ratio

Executive Summary

A prototype acoustic array for measurement of wind turbine noise has been designed in a collaborative effort by the National Renewable Energy Laboratory (NREL) and University of Colorado Boulder. The array is built upon 63 electret condenser microphones in a multi-arm logarithmic spiral pattern, a single calibrated B&K precision condenser microphone, in-house designed analog electronics, and an integrated National Instruments (NI) data acquisition system (DAS). Noise source maps are generated using a delay-and-sum beamforming algorithm with diagonal elimination in the cross-spectral matrix. The uniqueness of this array design over currently available commercial products is a lower frequency range, a weather-proof design allowing for long-term observational campaigns, and the ability to collapse and package the array for ease of transport.

After an initial deployment at the Northwind 100A research turbine site for system testing, the array was deployed in late 2012 at the upwind side of the Controls Advanced Research Turbine (CART)-2 at the National Wind Technology Center (NWTC). The turbine has a highly instrumented rotor and accompanying meteorological tower enabling noise correlations with both detailed turbine operational characteristics and atmospheric conditions. An active acoustic source has been used to calibrate the array and characterize its performance. Simulated point-source data have been used to compare these results to expected results. The array is shown to have a 3-dB beamwidth of 3.53 meters for a 750-Hz source at the center of the rotor, 56 meters from the center of the array. Turbine noise data have been collected over a range of operational conditions, including wind speeds from 7 to 22 m/s and rotor speeds of up to 42 rpm (6-second averages). Data from these measurement campaigns have been analyzed at frequencies from 750 Hz to 8 kHz.

The array in its current configuration has shown point-source localization accuracy on the order of a few tens of centimeters. However, a non-negligible variation in source location under various atmospheric conditions has also been observed. Compensation for sound convection using a simplified atmospheric model in the beam-forming algorithm improved the initial results but only approximately half of the position error was removed. A more robust atmospheric model could significantly improve the system's performance.

For the NWTC's CART-2, low frequency noise is dominated by mechanical noise in the nacelle and a squeek originating from the teeter-pin. Aeroacoustic noise near the blade tip dominates the higher frequency spectrum, typically observed on the downward passing blade. However, aeroacoustic noise has been observed on the upward passing blade during periods of significant yaw error in which the upward passing blade is operating at a higher angle of attack. An additional noise source was aparent over a range of frequencies below the rotor center and was thought to be blade-wake interaction with the tower or a scattering of blade noise off of the tower. This prototype array has been developed to a point where further study of these and other noise sources is now possible at NREL.

Table of Contents

List of Figures

1 Introduction

Acoustic arrays are implemented to remotely infer the location and strength of sources in an acoustic field. The arrays rely on signals from multiple microphones to deduce these spatial characteristics. Arrays have been used both in wind tunnels [1,2] and in the field [3,4] for measurements of noise from locomotives, airfoils, aircraft, and aircraft subsystems. However, relatively few studies have been conducted using these devices for measurements of wind turbine noise, particularly on full-scale turbines. Oerlemans et al. have conducted such a study in the Netherlands using an array of their design [4,5]. An array has been designed for the purpose of conducting similar research at the National Wind Technology Center (NWTC) outside of Boulder, Colorado.

This report discusses the design and use of a multi-arm, logarithmic spiral acoustic array by the National Renewable Energy Laboratory (NREL) for measurement and characterization of wind turbine-generated noise. The array was developed in collaboration with a team from the University of Colorado Boulder. This design process is a continuation of the elliptical array design work done by Simley [6]. A description of the array system design process is presented, including array shape design, mechanical design, design of electronics and the data acquisition system, and development of post-processing software. System testing and calibration methods are detailed. Results from the initial data acquisition campaign are offered and discussed. Issues faced during this initial deployment of the array are presented and potential remedies discussed.

2 Acoustic Array Design

The system design goals are described, and design strategy is discussed as it pertains to each of the array's constituent systems—mechanical, electrical, and software. The array construction process is described, including methods, necessary equipment, positional uncertainty, and positional tolerances.

2.1 Design Requirements

The NWTC required an acoustic array with several specific characteristics for further study of wind turbine acoustic emissions. First, to facilitate ease of deployment and use, the system has been designed to be fully weatherproof for sustainable, safe storage in the field. The system must be robust to withstand the expected conditions at the NWTC, including snow, rain, high wind and wind-borne debris, and temperatures between about -25°C and 40°C. With the design capable of operating under these conditions, the system can be left entirely assembled in the field for the vast majority of a testing campaign, greatly reducing experimental setup time.

In addition, it was desired that the array be capable of resolving relatively low frequency sources in turbine acoustic output. A benchmark frequency of 750 Hz was set, because this is approximately the low end of the blade trailing-edge noise spectrum [12]. The low-frequency capability of the array can be quantified by its main beamwidth in the plane of the turbine rotor, which scales with wavelength and, inversely, with array size. To reduce the main beamwidth and improve the resolution of the array, the array is significantly larger than commercially available products. For this reason, it has been designed and constructed in-house at the NWTC.

2.2 Array Shape Design

The array shape is a zero-redundancy, multi-arm logarithmic spiral layout. The shape was designed in an iterative process, based on the procedures outlined in Underbrink [7]. The shape is stretched in the streamwise direction to compensate for a chosen viewing angle of approximately 45° from the turbine hub. The stretching ratio of 2.25 provides improved vertical resolution, yet a feasible array size. Finally, in practice, the shape is rotated with its semi-major axis aligned with a point that is 65% of the length of the rotor radius from the hub on the side of the downward-passing blade. The stretching and pointing adjustments are in accordance with the methods of Oerlemans et al. [4].

The resulting shape consists of 7 spiral arms each with 9 elements as shown in Figure 1, giving a total of 63 array elements. The performance of the array is characterized using simulation of an ideal, single-frequency (1-kHz) point-source in the rotor plane. This simulation provides a visualization of the array point spread function (PSF) as shown in Figure 1, as well as an analytical tool for determining the beamwidth and sidelobe levels and locations. Figure 2 shows the array beamwidth at the hub location as a function of frequency.

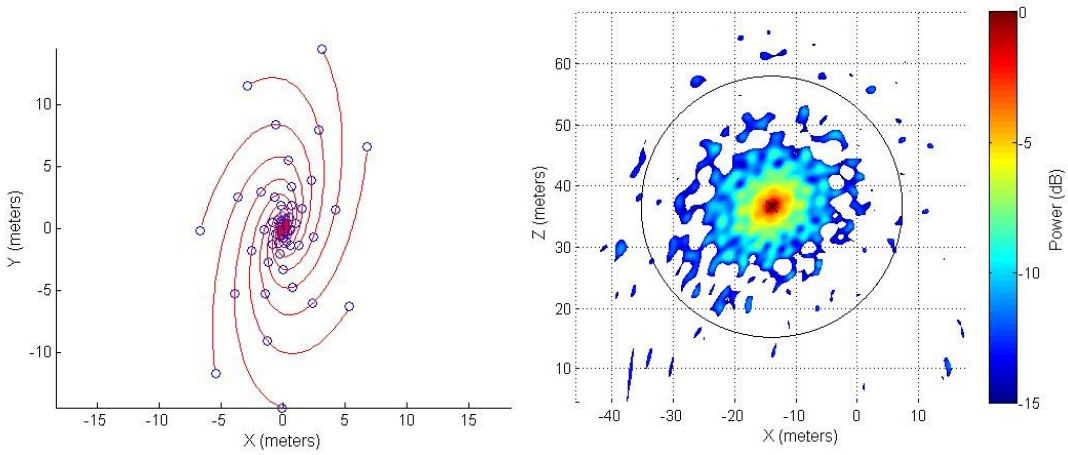

Figure 1. Nominal array shape (left) and point spread function of the design for a 1-kHz point source at the hub of the Controls Advanced Research Turbine (CART)-2 (right). The circular outline represents the blade tip swept curve of the CART-2. Note that X, Y, and Z are in the cross-stream, downstream, and vertically upward directions, respectively.

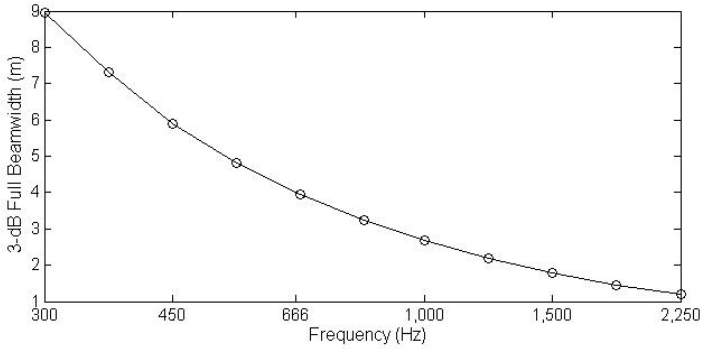

Figure 2. 3-dB full beamwidth of the array versus frequency at a range of 56 meters and elevation angle of 42°

Figure 2 shows that, as expected, at frequencies well below 750 Hz the array resolution is relatively coarse. At 750 Hz, the array has a 3-dB beamwidth of 3.53 m. This beamwidth does not allow for high-precision resolution of noise sources. It does, however, allow for separation of noisy regions, such as nacelle noise from noise near the blade tips.

2.3 Electronics and Data Acquisition Hardware

A block diagram of the signal path and data acquisition system (DAS) is shown in Figure 3. The system utilizes 63 Panasonic WM-64BC electret condenser microphones. Because this particular model was discontinued after the design was completed, several channels now utilize PUI Audio POM-2242P-C33-R electret condenser microphones. The two models are electrically and geometrically similar, and the difference in sensitivity is compensated for by calibration.

The microphone signal is amplified in two stages. The first is a differential amplifier, based on a bipolar junction transistor (BJT). The amplifier is powered by a DC voltage provided by the second amplification stage. This amplifier puts out a differential signal and is located only several centimeters along the wire from the microphone for improved signal-to-noise ratio

(SNR). The amplifier is built upon two BC857B PNP transistors. The second stage is a differential to a single-ended, non-inverting, op-amp-based amplifier with a gain of approximately 220. This stage utilizes two NE5532 op-amp ICs. The two stages are connected by 30 meters of 2-conductor, shielded cable.

The 63 signals are then passed to an integrated National Instruments (NI) DAS. The DAS is composed of four, 16-channel NI PXIe-449 modules and a PXIe-8108 controller. Each module has a resolution of 24 bits and is capable of simultaneous sampling. A sampling rate of 25 kHz was chosen to reduce the size of data files. The resulting Nyquist frequency of 12.5 kHz is sufficient for our interest in low frequency content. The modules' anti-aliasing filters were applied to the incoming signals and are automatically set to the Nyquist rate.

A B&K 4189 precision microphone was positioned in the inner section of the array as a reference signal. This microphone is calibrated with a 94-dB signal at 1 kHz using a Brüel & Kjær 4231 calibration source. The reference signal is then passed to an NI-9233 USB DAQ card, which is also sampled at 25 kHz and anti-alias filtered. The signal is not sampled simultaneously with the array signals, but the lag was shown to be less than 0.06 seconds.

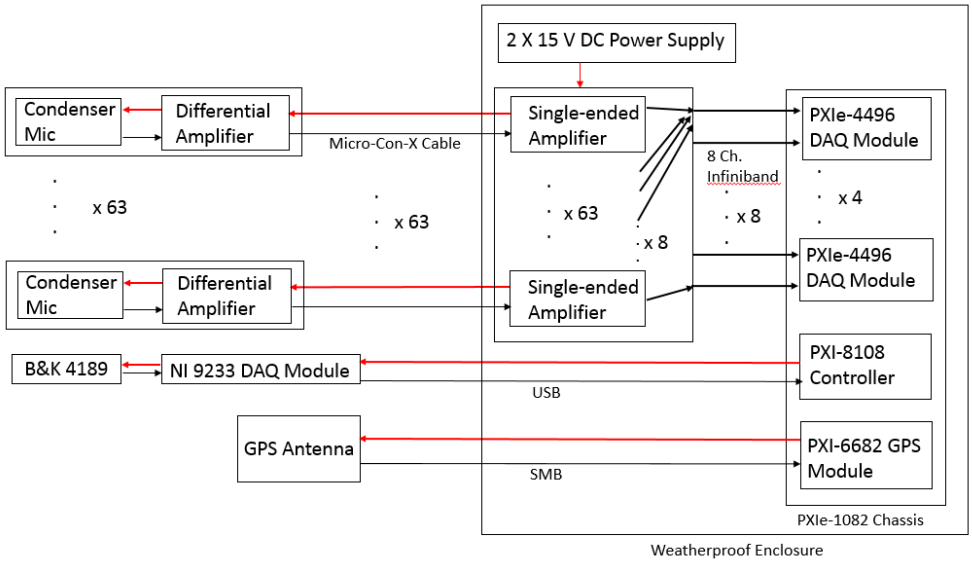

Figure 3. Block diagram of the microphone electrical hardware. Black arrows represent signals/data and red arrows represent power.

Finally, to synchronize the array measurements with the instrumentation data from the turbine, a NI PXI-6682 GPS module is used to timestamp all data. This allows for accurate correlation of noise data to atmospheric conditions and turbine operational parameters.

2.4 Field Hardware

The array's structural design is based on two segments: the fixed, inner array, which contains between four and five elements of each spiral arm, and the modular outer array. See Figure 4. The inner array is built from 80/20 aluminum extrusions supporting a laser-cut plywood top sheet. The frame is secured by four rebar stakes, each penetrating approximately 18" into the earth.

The modular outer array elements are each placed on laser-cut, circular plywood mounts with a diameter of 0.56 m and a thickness of 13 mm. The mounts are laid flat and surrounded by a dirt-mortar mix to minimize edge-scattering effects. The dimensions of the modular element mounts are based on recommendations of international standard IEC 61400-11 [8], though the diameter was reduced from the recommended 1 m to 0.56 m for convenience. The recommendation of 1-m diameter is to allow analysis of frequencies as low as 20 Hz, whereas this array's analysis does not examine frequencies below 750 Hz. A simple scaling with wavelength implies that 0.56 m will be sufficient for accurate prediction of pressure-doubling effects.

Each microphone was placed using an analog survey transit to within approximately 10 cm of the designed location. The microphone's coordinates were then measured using an Automated Precision Inc. Tracker3 laser spatial analyzer to an accuracy of roughly 1 mm in each direction, and these coordinates were used for beamforming.

(a)

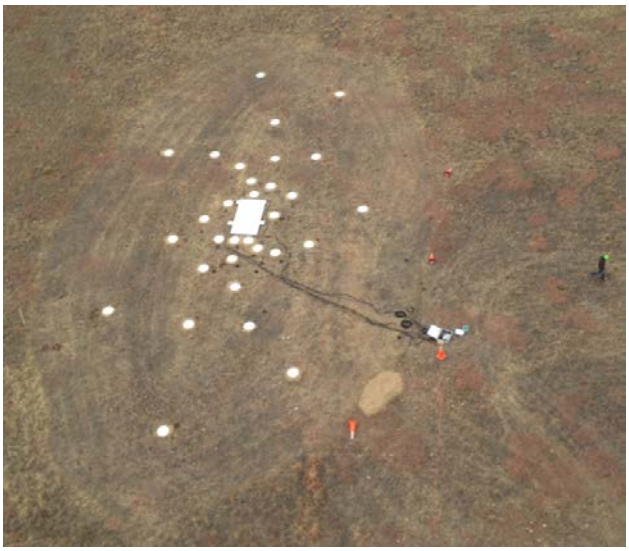

(b)

(c)

(d)

Figure 4. Sixty-three microphone arrays deployed on the CART-2 turbine at the NWTC (a); view of the array from the CART-2 nacelle (b); inner, fixed array structure (c); and outer, modular array element (d). ***Photo (a) by Mike Asheim; Photos (b) through (d) by Jason Roadman, NREL***

2.5 Weatherproofing

The microphones are mounted on the outside of a waterproof, polycarbonate box approximately 5 cm on a side that is rated for NEMA-4 water ingress. See Figure 5. The microphone wires are sealed with a waterproof silicone adhesive. The first amplification stage differential amplifier electronics are housed within each of these small enclosures. Waterproof Micro-Con-X connectors produced by Conxall utilize rubber washers to maintain the waterproof integrity of the box. Custom cabling by the same manufacturer provides the signal path from each microphone to the central data acquisition enclosure. Note that the nominal design and IEC standards call for the use of wind screens, though these were not present during the initial data acquisition campaign because of time constraints. Hemispherical, 90-mm diameter wind screens will be manufactured from spherical, ACO Pacific outdoor wind screens and included in the future deployments.

The data acquisition hardware is enclosed in a large aluminum enclosure. It is 75 cm x 105 cm x 30 cm in size and is large enough to house the second-stage amplification boards, power supplies, and the National Instruments PXI data acquisition (DAQ) chassis. All hardware inside the chassis is either bolted directly to the backplane or mounted on DIN rails. Micro-Con-X connectors provide the corresponding waterproof signal path into this enclosure from each microphone. The Ethernet and 120Volts (V) AC power connections use a similar waterproof connector. An electric heater is mounted inside the enclosure to act as a dryer and dehumidifier for condensation during diurnal thermal cycling.

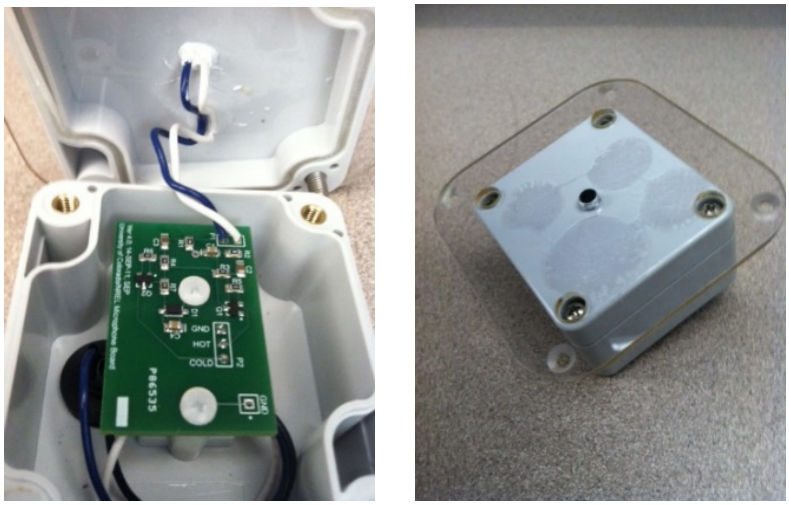

Figure 5. Microphone electronics waterproof enclosure and mount (left) and contained differential amplifier (right)

(Photo by Steve Buck, University of Colorado Boulder)

2.6 Data Acquisition and Beamforming Software

The data acquisition software has been developed in Labview for seamless integration with the PXI DAQ hardware. The software simultaneously samples the 63 array channels as well as the reference microphone (not simultaneously). The software also enables the PXIe-4496 modules' anti-aliasing filters and reads a timestamp from the PXI-6682 GPS module. All of these

features—simultaneous sampling, reference microphone calibration, anti-alias filtering, and GPS timestamping—have been verified on an individual basis.

The beamforming software is written in Matlab and implements a traditional frequency domain delay-and-sum algorithm. Frequency domain implementation improves the speed of the code's execution over the analogous time domain algorithm [6]. The diagonal elements of the cross-spectral matrix are nulled for reduction of the effects of microphone self-noise and electrical noise. Beamforming is typically performed on 6-second sections of data, averaging the effects of between three and four full rotor rotations. The averaging time is reduced or increased based on the consistency of atmospheric conditions.

The software compensates for the effects of sound convection by assuming a constant, identical wind speed and direction between the microphone and scan location, as in [2,3] and based on the geometrical convection analysis of Soderman et al. [9] extended to three dimensions. The merit of this method was tested and is discussed in Section 4.2.

3 Field Testing and Calibration

After testing on a component-by-component basis, the full array system was deployed at the Northwind 100A turbine at the NWTC. A controlled active acoustic source was used to assess the performance of the array, and recorded data were compared to simulated, ideal data. A description of the testing conditions and methods is given here, along with a recommended array calibration method.

3.1 Active Source Testing

The complete array system has been tested using a controlled, active acoustic source in a known location. The source's location is measured by one of two methods—initially, by using an analog surveying transit, and in later tests with a digital Automated Precision Inc. Tracker3 coordinate-measuring machine (CMM) for improved accuracy. The survey transit indicates the source location to within an estimated 71 cm in each direction. The CMM, on the other hand, provides an accuracy of approximately 1 mm. The measured location is then compared to the noise maps generated by the beamforming software. The acoustic signal for the first testing campaign is generated using the sound function in Matlab and amplified using a Fender, 15-Watt "Rumble 15" bass guitar amplifier. This setup provides both the flexibility and power required for the purposes of these tests. The latter active source testing was conducted with a custom-designed acoustic source formulated around a 3.5-kHz pure tone speaker.

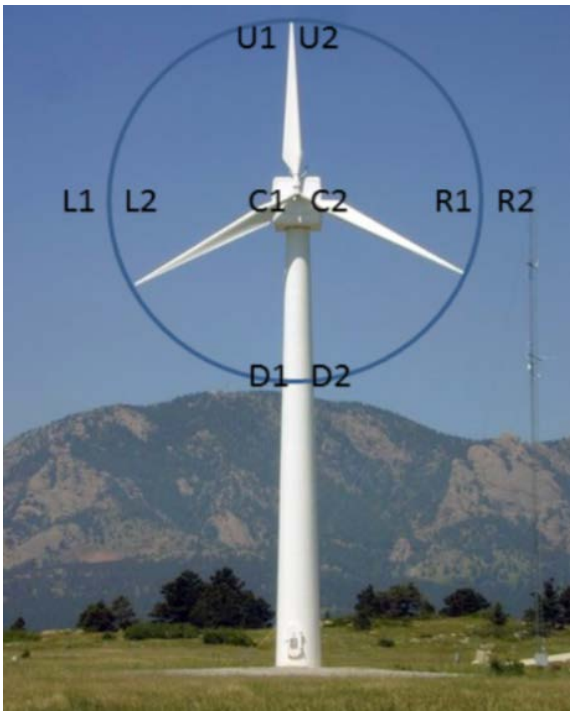

Figure 6. Spatial locations of acoustic source for array system testing
(Photo by Steve Buck, University of Colorado Boulder)

The initial active source test of the array consists of a matrix of ten spatial locations and three acoustic signals—1.5 kHz and 3.2 kHz pure tones and a broadband signal. The spatial locations are spread throughout the rotor swept region of the Northwind 100A turbine at the NWTC as

shown in Figure 6. With the turbine shut down, a hydraulic platform lift was used to raise the source to each of the lettered regions U, D, L, R, and C (up, down, and so on). The source was then moved from the left side of the platform to the right side, denoted by the numbers 1 and 2. The nominal spatial locations are based on analog survey transit measurements, which hold approximately 71 cm of uncertainty in each direction. The relative distance between positions 1 and 2 in each region is also verified by tape measure, which gives higher precision information for comparison to noise-map results.

The size of this test matrix lends itself to a statistical description of results. Data were recorded for 90 seconds for each of the three signals for each of the ten locations. The data are broken into six-second sections for beamforming. This gives a total of fifteen, six-second data segments for each signal and location.

Averaging over all 150 1.5-kHz data sets, a mean position error exists. This error is defined as the absolute discrepancy between surveyed position and noise-map maximum power location. In this case, the mean position error is 77.4 cm. At 3.2 kHz the mean error is 84.8 cm. The standard deviations in noise-map maximum power location at 1.5 kHz and 3.2 kHz are 25.1cm and 32.9 cm, respectively. Finally, the mean absolute error in relative distance between positions 1 and 2, averaged over all five regions, was 19.5 cm for the 1.5-kHz source and 12.9 cm for the 3.2-kHz source. The latter result suggests that the magnitude of error in position versus surveyed position is greatly influenced by the uncertainty in surveying data, which was estimated at 71 cm.

Broadband signals were analyzed by the beamforming software over third-octave bands centered at about 1.5 kHz and 3.2 kHz. Results hold similar standard deviations between measurements, but the mean absolute error is approximately double. This deviation is likely due to the fact that the same broadband signal was repeatedly used, so the noise would logically result in a consistent error between subsequent measurements.

The preceding results, along with a qualitative comparison of experimental noise maps to simulation results as in Figure 7, signify that the array and associated software are functioning properly. Wind speeds varied between 2 and 6 m/s during these speaker tests and are not taken into account in these noise maps.

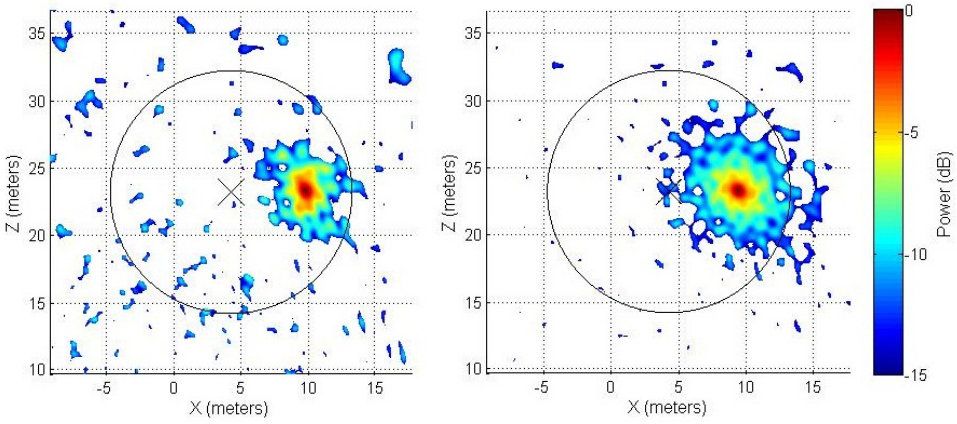

Figure 7. Noise maps generated for experimental data (left) and simulated point-source data (right) for a 1.5-kHz source at location R1

The variation in location of maximum power in the noise maps suggests that atmospheric conditions have significant influence on the accuracy of beamforming. Specifically, it is noted that variation in noise maps occurs on a longer time scale than can be explained by motion of the hydraulic lift's boom and the source. Figure 8 shows the vertical coordinate of the location of maximum power for seven consecutive 6-second sections of array data for a 3.2-kHz source at location U2. Note that the standard deviation for these six sections of data is 98.1 cm, which is substantially higher than the overall standard deviation of 32.9 cm. The systematic variation in the vertical coordinate over this 36-second section of data may logically be explained by a variation in atmospheric conditions, because it is not uncommon for wind conditions to vary significantly on these timescales. This variation cannot be verified definitively for this case, however, because no real-time wind data are available.

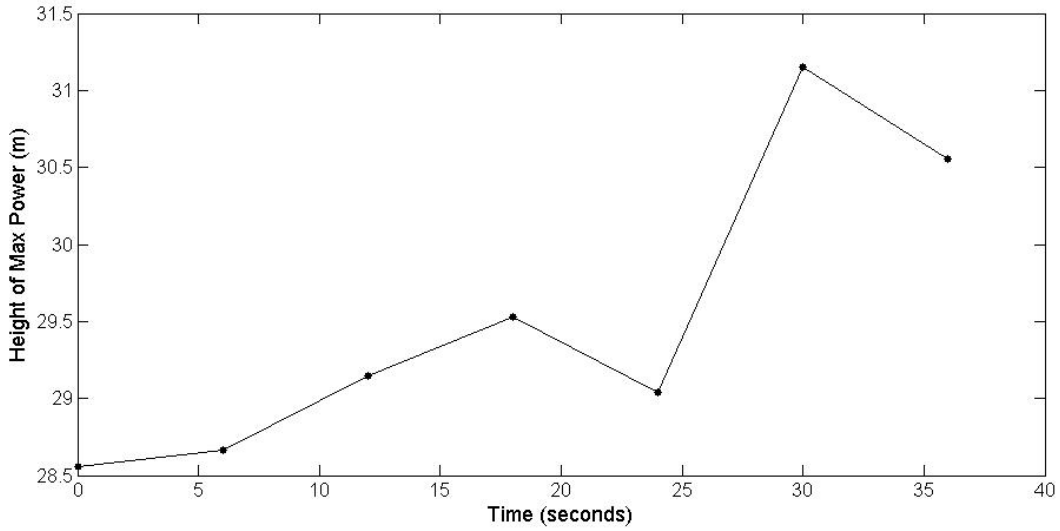

Figure 8. Vertical coordinate of the location of maximum power in seven consecutive 6-second sections of array data. Source frequency of 3.2 kHz at location U2. Nominal vertical coordinate is 28.7 m.

To investigate the claim that atmospheric conditions are responsible for the appreciable errors in beamforming results, further experimentation has been conducted in which other potential sources of error—source location uncertainty, wind condition uncertainty, and acoustic scattering—are eliminated or reduced. The source used during these tests is designed to minimize non-local, coherent acoustic generation, and is shown in Figure 9. The acoustic dampening foam shown is used to prevent vibrational acoustic generation by the mount and edge scattering off of the mount. The L-shaped profile of the mount is designed to block the line of site from the source to the turbine that the source is fastened to, thus minimizing scattering off of the turbine. The location of the source is known to within approximately 15 cm, because the location of the turbine relative to the array has been measured with the Tracker3 spatial analyzer, and the turbine geometry is well known. Finally, wind speeds during experimentation are measured via local anemometry and time-referenced to GPS.

Figure 9. Isolated point source design. The speaker circled in red emits a 3.5-kHz pure tone.
(Photo by Steve Buck, University of Colorado Boulder)

Testing has been conducted using this source at the CART-2 turbine facility under wind conditions below 3 m/s. Beamforming is performed on ten 6-second sections of data with an overall average wind speed of 1.21 m/s. The mean absolute error in location of maximum power versus nominal source location is 45 cm. The standard deviation is 26 cm. Note that the range of the source for these tests is 59 m from the center of the array—approximately double the range for the tests conducted at the Northwind 100A site.

3.2 Array Calibration

To compensate for the amplifier gains and microphone sensitivities of each channel, a weighting factor for each signal is included. Dougherty's suggested method [10] involves the derivation of a complex weighting that corrects both amplitude and phase, with phase corrections aiding the imperfect knowledge of microphone location. Microphone locations were measured within an accuracy of approximately 1 mm. This is less than 1/16th of a wavelength for frequencies up to about 16.7 kHz, which is well beyond the range of the analyses of this work. Microphone location errors of this magnitude should cause minimal detriment to beamforming, according to the work of Simley [6], and thus our calibration corrects only for amplitude.

An active acoustic source is used for calculation of the weights for each channel. The speaker is placed in the far field of the array and located using the Tracker3 laser spatial analyzer. A pure tone acoustic signal at 500 Hz is generated and recorded in several 45-second sections of data. The signal is the dominant signal in the acoustic field, with an SNR of approximately 45 dB above adjacent frequencies. Atmospheric attenuation at this frequency is less than 0.5 dB over

the range of the array [11] and is neglected. A fast Fourier transform (FFT) of the data from each channel is taken in blocks of 1,000 samples and averaged over a sufficiently large span of data. The relative magnitudes of each signal are then adjusted for range from the source and normalized to the sensitivity of the reference microphone.

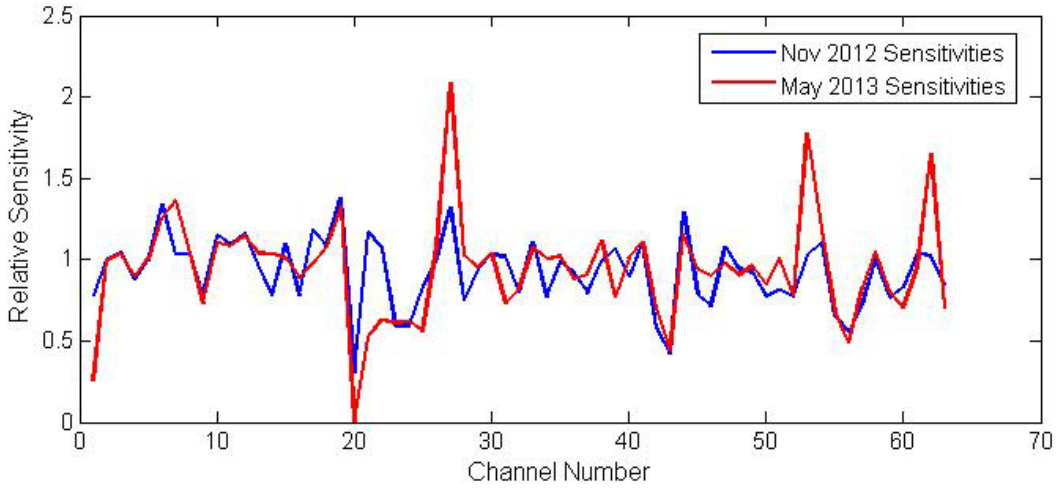

Figure 10. Channel sensitivities relative to channel 2 at deployment of the array versus relative channel sensitivities after the winter season

This method also allows for investigation of the weather-readiness of the field equipment. Figure 10 shows the relative sensitivity of each microphone at the deployment of the array in November 2012 and the sensitivities as of May 2013. Microphone boxes were left in the field through the interim period. The comparison illuminates several notable facts. The first is that microphones 1, 20, 21, and 22 had degraded signals, with microphone 20 being nearly out of commission. It was found that the silicone seal was faulty on these microphone boxes and moisture was present inside.

Also notable is the significantly increased sensitivity of channels 27, 53, and 62 after the winter season. This is not likely attributed to electronics, but potentially caused by degradation of the module elements' sand-mortar edge treatment. Edge scattering effects may have caused a standing wave condition on the surface of the circular microphone mounts, affecting the strength of the received signal. This hypothesis must be investigated further, however. Plans are in place to improve the durability of edge treatments.

4 Turbine Noise Data

A data acquisition campaign was conducted at the CART-2 facility at the NWTC from November 2012 to August 2013. In this section, the experimental setup and available instrumentation are described, the turbine operational conditions and atmospheric conditions for which data were gathered are detailed, and selected results are presented and discussed.

4.1 Experimental Setup and Instrumentation

The array has been deployed since late 2012 on the westward side—typically upwind—of the CART-2 at the NWTC. The turbine is a modified, two-bladed Westinghouse WWG-0600 machine rated at 600 kW. It has a hub height of 36.4 m and a blade-tip radius of 21.3 m. The rotor operates upstream of the tower.

Instrumentation on the turbine and in the surrounding area provides turbine operational data and atmospheric condition data sampled at 400 Hz and synchronized with GPS time signals to within a millisecond. Available operational data include, but are not limited to, nacelle yaw position, rotor azimuth and rotational rate, individual blade pitch angles, and the tilt of the rotor with respect to vertical. Available atmospheric conditions include wind speed and direction at the hub height, top of the rotor, and bottom of the rotor; temperature; and barometric pressure.

The array is located with its center approximately one hub height from the rotor plane. The array's semi-major axis aligns with a point 65% of the distance from the hub to the blade tip on the downward-passing blade under nominal wind conditions. The reference microphone is placed on the inner array platform at a point that is 32 cm from the nearest array element and 37 cm from the edge of the platform. This microphone is placed in a hemispherical, 16-cm-diameter wind screen.

4.2 Data Acquisition Campaign

Since deployment in November 2012, 380 turbine noise datasets have been acquired using the array over a range of wind speeds during field experimentation. Data were taken over 45 second periods and split into 6-second-average segments for further analysis. Wind speeds present in the data span the range from 8 m/s to 22 m/s, covering from the low-speed cut-in up to 88% of the high-speed cut-out of the turbine. Rotor speeds ranged from 15 to 42 RPMs, effectively covering the operational range of the turbine. Data were acquired with the turbine in a feathered position during similar wind conditions for spectral comparisons.

Preliminary analysis of the data reveals several notable characteristics. The first is an unexpected positional offset, primarily in the vertical direction between the expected location of both mechanical and aerodynamic noise sources, and the locations observed in noise maps. This is discussed further in following paragraphs. The second notable characteristic is the tonal "squeaking" noise caused by the teeter pin of the turbine, which is located at the junction of the two blades. This source has been observed at frequencies between approximately 0.8 and 1.1 kHz. It is generally a very pure tone, which has the benefit of helping to characterize the vertical offset observed.

As discussed in Section 2.6, the beamforming software compensates for sound convection by assuming a constant wind velocity between scan locations and the microphones. Figure 11 shows

noise maps for 0.8 kHz—nearly the exact frequency of the teeter noise for this dataset—with and without this compensation. An FFT of the signal shows that the teeter noise has an SNR of about 10 dB above adjacent frequencies. The convection model improves the result by 64 cm in the X-direction and 4.8 meters in the Z-direction. Note that in this particular dataset there was a yaw error of 36° between the rotor-normal and the wind direction, with wind direction rotated counter-clockwise as viewed from above, which explains the correction in the X-direction.

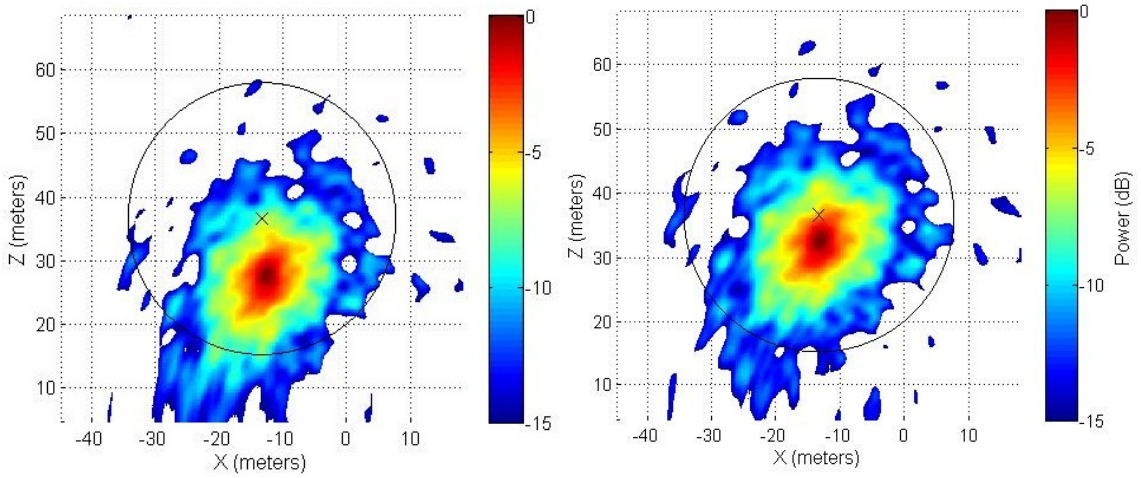

Figure 11. Noise maps for data with 800-Hz teeter noise without (left) and with (right) convection correction. The cross hairs represent the nominal location of the teeter pin. The X-direction is horizontal in the plane of the rotor, and the Z-direction is vertical. The average wind speed is 17.21 m/s. The average yaw error angle is 36°, counter-clockwise as viewed from above.

Having been measured with the laser tracker, knowledge of the location of the teeter pin and its relation to the array is precise, and the assumed location error cannot account for the offset shown above. It is therefore apparent that the atmospheric model used is not yet sufficient, because an error on the order of four meters is still present after its implementation. The remaining error is attributed to the wind shear profile and turbulence refraction, neither of which is accounted for. This claim is supported by the absence of this error in the results of speaker testing under low wind conditions.

Whereas the teeter noise, when present, dominates the frequency regime just below 1 kHz, trailing-edge noise is readily viewed in the regime of 3.2 kHz. Downward-passing blade noise is dominant for the majority of data, similar to the results of Oerlemans [2,3], and attributed to convective amplification and source directivity of trailing-edge noise. Application of the convective correction algorithm improves results for trailing-edge noise, as shown in Figure 12. The corrective technique was particularly effective for this dataset. It is noted that the correction is still imperfect: The dominant noise source in this case is likely trailing-edge noise near the blade tip [5], but it is apparent in the figure that the region of the noise map swept by trailing-edge noise does not coincide with the physical location of the outer blade region.

It is also noted that the correction is not always this effective. Figure 13 shows a case where the uncorrected noise map is distorted relative to the expected semicircular pattern. When pure convective effects are removed, the noise map is still significantly distorted. This effect has not yet been well correlated to any specific atmospheric condition and requires further analysis.

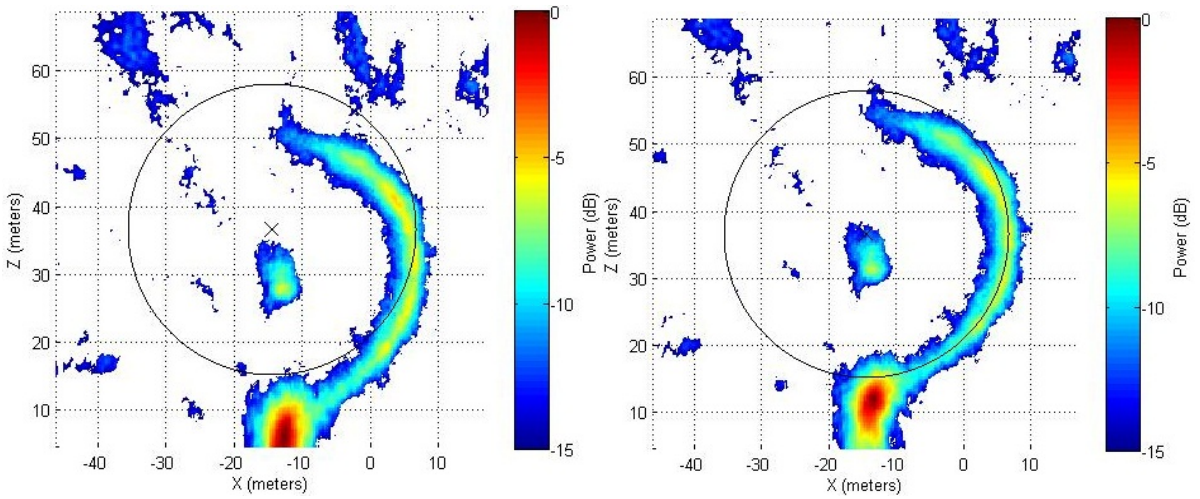

Figure 12. Noise maps for wind turbine noise in the 3.2-kHz one third-octave band without (left) and with (right) convection correction. The average wind speed is 16.37 m/s. The average yaw error angle is -1.57°, counter-clockwise as viewed from above.

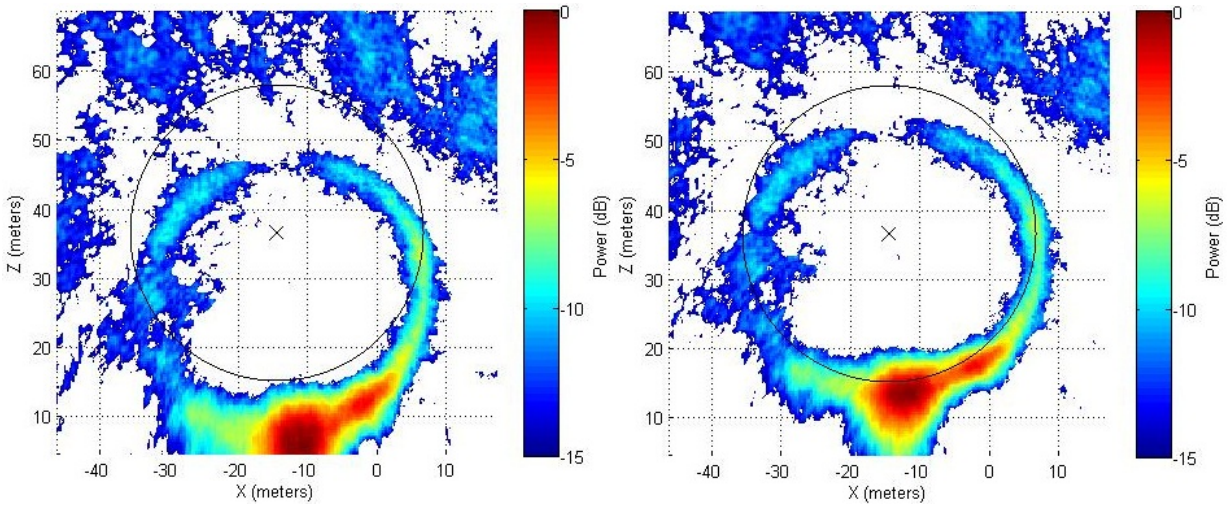

Figure 13. Noise maps for wind turbine noise in the 3.2-kHz one third-octave band without (left) and with (right) convection correction. The average wind speed is 15.41 m/s. The average yaw error angle is -2.15°, counter-clockwise as viewed from above.

In some cases the blade-tip noise was dominant on the upward passing blade, which is contrary to the predicted effects of convective amplification. Analysis based on five observed cases of this noise-map characteristic (6-second averages), points to a potential association with yaw error—or angular difference between wind direction and the rotor-normal direction—above about 20°, with the wind direction rotated counter-clockwise as viewed from above (causing an increase in angle of attack of the blade as it sweeps out the lower portion of the rotor). Further investigation is required to verify this definitively. Figure 14 shows two noise maps for third-octave bands that are centered at 3.2 kHz, one with downward-passing blade noise and one with upward passing blade noise.

Finally, it was noted that the apparent noise source in the noise maps of Figures 12, 13, and 14 just below the center of the rotor is present over a frequency range from about 1 kHz to 6 kHz.

This is potentially a blade-wake turbulence interaction with the tower or scattering of blade noise off of the tower. It is not likely caused by blade-tower-interaction noise, because this is typically very low frequency and not prevalent in upwind turbines [12]. This phenomenon will be investigated further.

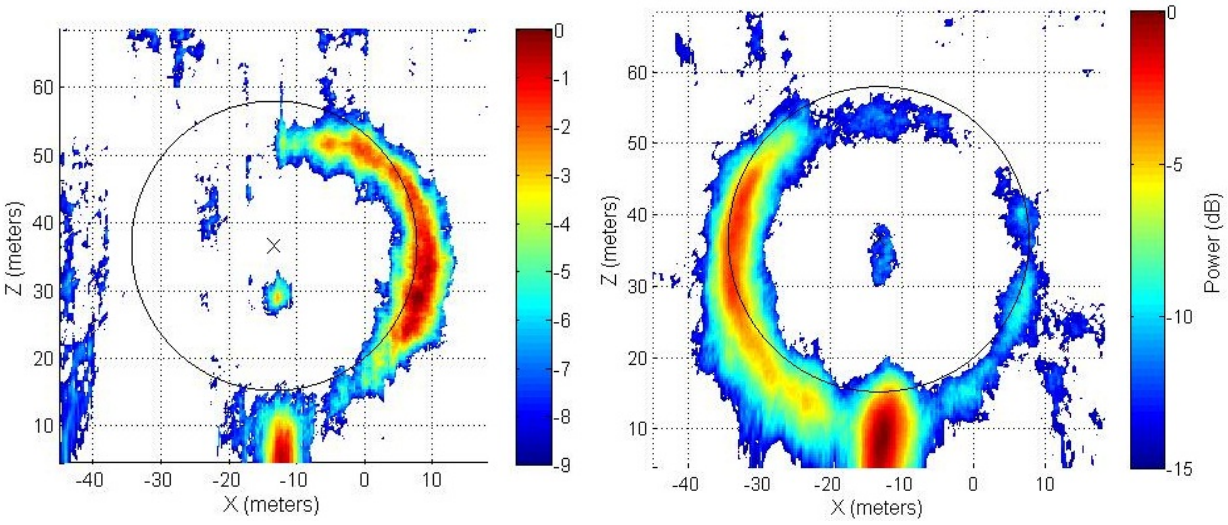

Figure 14. Noise maps for third-octave bands centered at 3.2 kHz. A wind speed of 16.4 m/s and yaw error of 2.1° (left) and a wind speed of 16.8 m/s and yaw error of 31.3° (right), both counter-clockwise as viewed from above.

5 Future System Improvements

Future improvements to the array system will be implemented such that the array may be left in the field without incurring damage from water, local wildlife, and extreme temperatures. While the system is currently partially weatherproof, it is not yet fully so. In addition, several improvements will be implemented purely for convenience and ease of use. Finally, atmospheric modeling will be a primary focus of future research, with the objective of understanding and minimizing errors in beamforming caused by atmospheric conditions.

5.1 Mechanical Improvements

After deployment in the field for almost 2 years, several lessons have been learned about the durability of the individual components. Future improvements in these areas could further improve the robustness of the array.

In this current version of the array, all acoustic surfaces were laser cut out of high quality plywood and painted with a durable epoxy-based paint. Though this method worked well, the paint is starting to crack around the plywood edges after two years. To improve the lifespan of the acoustic surfaces, a non-organic-based substrate could prove beneficial. Utilization of a laser-cut, opaque, white acrylic would enable the array to better stand up to UV and weather. It would cost more as a raw material, but save significant labor time on the fabrication side because it would not need to be painted. Also, the mounting holes for the microphones can be directly tapped, so threaded brass inserts wouldn't be required.

The array would also benefit from improved cable organization. Sixty-three individual cables laid out between the microphones and the DAS box were difficult to keep organized. Replacing failed cables only exacerbated this problem. A future cabling scheme might include individual distribution boxes in the interior of the array—one near the inner array and one partway out along each semi-major array axis. Cables from microphones that are near each other could be grouped together as they approach the distribution box. Then, a single armored cable could be run between each distribution box and the DAS box located on the perimeter of the array.

Additionally, the array cabling was chewed by rodents several times throughout the deployment. This problem could be mitigated in future deployments in two ways. First, the inner array should be protected from rodents burrowing underneath it by utilizing a wire mesh attached along its perimeter and buried under the dirt mixture used to smooth the surrounding terrain with the top of the acoustic surface. This mesh should extend out away from the array a distance of approximately 0.5 meters. Second, the individual cabling should be armored wherever possible. This additional protection would be achieved using a combination of traditional electrical conduit, true armored cable (likely for the runs between future distribution boxes and the DAS as mentioned), and a braided metal sleeve over portions of the cable.

Several final modifications must be made to the DAS enclosure's ventilation system to allow extended deployment of that portion of the system at the NWTC. Air circulation must be maintained between the enclosure and the ambient air to provide sufficient cooling for the enclosed electronics. The enclosure is equipped with a fan that draws air into the bottom of the chassis and exhausts at the top through hooded inlet ducts. The edges of these hoods should be

waterproofed with aluminum tape and the hoods extended sufficiently far below the exhaust vents so that moisture will not be blown back into the enclosure by strong winds in a rain storm. Additional protection from water ingress through the exhaust hoods will be provided by spring-loaded baffles that seal on weather-stripping when the cooling fan is not operating.

As data is not being acquired continuously, the exhaust fan in the DAS enclosure could be commanded through software to shut down during the 45 seconds that data are being collected on the array to reduce background noise interference, and then turned back on again once the individual measurement is complete. A watchdog function could be included to disable this feature when the interior of the enclosure rises above a certain temperature whereby shutting down the fan would put the PXI at risk of overheating.

Finally, the waterproofing of the individual microphone boxes must be improved. Water and condensation were periodically found within these enclosures. It is thought that the moisture ingress was caused by cracks in the sealant between the microphone and the enclosure. The cracking was likely caused by exposure to the elements for extended periods of time. Efforts to reduce this ingress should focus on finding a better sealant, perhaps of the high-temperature RTV type. Furthermore, use of desiccant within each box would mitigate the negative effects of any trapped moisture.

5.2 Atmospheric Modeling

As described previously, performance of delay and sum beamforming without consideration of the conditions in the medium between acoustic sources and sensors—i.e., atmospheric conditions in the vicinity of the array—results in erratic behavior and appreciable errors in noise-map characteristics. The study of the aeroacoustics of wind turbines relies heavily on the accuracy of measurements under a broad range of atmospheric conditions. Therefore, understanding these conditions is pivotal to scientific analysis of data. As has been detailed, the correction for convective effects improved results significantly, but errors are still present—in some cases more than others. It is believed that shearing effects and temperature stratification in the atmospheric boundary layer and turbulence diffraction are the currently unmodeled physical phenomena of the most significant consequence.

As a first priority, the effects of the shearing structure in the boundary layer will be analyzed. This is because the instrumentation at the CART-2 facility provides significant information about the shearing structure. Wind shear affects beamforming results caused by the diffraction of acoustic waves through the sheared medium. This diffraction, in turn, affects the path length traveled between source and sensor and the measured phase offset. The complexity of the issue should not be understated, because the effective path length will need to be calculated for each sensor and each scanned location—approximately 2.5 million path lengths for the current configuration. The calculations must then be accurate as well as efficient.

6 Conclusions

The array described in this paper is designed for measurement and localization of wind turbine noise. A performance analysis based on active acoustic source testing shows an accuracy of point-source localization on the order of a few tens of centimeters. A non-negligible amount of noise-map variation with atmospheric conditions was observed in both speaker tests and turbine noise data. Implementation of compensation for sound convection helped this matter, removing approximately half of the offset in either direction for the case discussed. However, a more robust atmospheric model could still significantly improve the system's performance. Initial turbine noise data analyses show that mechanical noise in the nacelle, and particularly teeter-pin squeak, dominates the relatively low frequency output. With increased beamforming frequency, the relative strength of aeroacoustic noise near the blade tip dominates, and is typically observed on the downward-passing blade. Aeroacoustic noise near the blade tip has also be observed on the upward passing blade, typically when the turbine is operating with significant yaw error in which the upward passing blade is operating at a higher angle of attack.

References

1. Bahr, Christopher. Assessment of Trailing Edge Noise Measurement Techniques. University of Florida, Department of Mechanical and Aerospace Engineering. 2010.
2. Koop, L., Ehrenfried, K. "Microphone Array Processing for Wind-Tunnel Measurements with Strong Background Noise". 14th AIAA/CEAS Aeroacoustics Conference, AIAA 2008-2907. Vancouver, British Columbia. May 2005.
3. Zhang, X., Xiao, Y. G., Deng, H. L. "Noise Source Localization Investigation in High Speed Train Based on Microphone Array". Applied Mechanics and Materials, Vol. 103. 2011.
4. Oerlemans, S., Lopez, B. M. "Acoustic Array Measurements on a Full Scale Wind Turbine". 11th AIAA/CEAS Aeroacoustics Conference, AIAA 2005-2963. Monterey, California. May 2005.
5. Oerlemans, S., Schepers, J. G. "Prediction of wind turbine noise and validation against experiment". International Journal of Aeroacoustics, Vol. 8, No. 6, 2009.
6. Simley, E. Development of an Acoustic Array for Wind Turbine Aeroacoustic Noise Analysis. Master's thesis. University of Colorado Boulder, Department of Electrical, Computer, and Energy Engineering. 2010.
7. Underbrink, J. R. "Aeroacoustic Phased Array Testing in Low Speed Wind Tunnels". Aeroacoustic Measurements. Edited by Thomas J. Mueller. Springer 2002.
8. IEC Norm 61400-11. "Wind turbine generator systems – Acoustic measurement techniques" (2002).
9. Soderman, P. T., Allen, C. S. "Microphone Measurements In and Out of Airstream". Aeroacoustic Measurements. Edited by Thomas J. Mueller. Springer 2002.
10. Dougherty, R. P. "Beamforming in Acoustic Testing." Aeroacoustic Measurements. Edited by Thomas J. Mueller. Springer 2002.
11. Blackstock, D. T. Fundamentals of Physical Acoustics. John Wiley and Sons, New York, 2000.
12. Wagner, S., Bareiß, G., Guidati, G. Wind Turbine Noise. Springer 1996.